Emergence of Anionic Counterparts of Divalent Metal Salts as the Fine-Tuners of Alginate Hydrogel Properties for Tissue Engineering and Drug Delivery Applications

Subhasis Dash[1,#], *Pavan Gutti*[1,#], *Birendra Behera*[2], and *Debasish Mishra*[1,*]

Abstract:

The role of anionic counter ions of divalent metal salts in alginate gelation and hydrogel properties was thoroughly investigated. Three anions were selected from the Hofmeister series viz. sulphates, acetates and chlorides paired in all permutations and combinations with calcium, zinc and copper divalent metals. Spectroscopic analysis revealed the presence of anions and their interaction with the metal atoms post-gelation. Data showed gelation time and other hydrogel properties were mostly governed by the cations. However, subtle yet significant variations in viscoelastic, water-uptake, drug-release and cytocompatibility properties were anion dependent in a cationic group. Computational modelling study showed metal-anion-alginate configurations were energetically more stable than metal-alginate models. The *in vitro* and *in silico* studies conclude that acetate anions precede the chlorides in the drug-delivery, swelling, and cytocompatibility fronts, followed by sulphate anions in each cationic group. Overall, the data provided affirmation that anions are integral part of the metal-alginate complex. Furthermore, anions offer a novel option to further fine-tune the properties of alginate hydrogels for tissue engineering and drug delivery applications. Moreover, extensive exploration of this novel avenue would enhance the usability of alginate polymers in pharma, environmental, biomedical and food industries.

Keywords: Biomaterials; Alginate; Anions; Hydrogel; Drug release; Density function theory (DFT) simulations

---

Authors' Affiliations:

[1.] Bioinspired Design Laboratory, School of Biosciences and Technology (SBST), Vellore Institute of Technology (VIT) Vellore, Tamil Nadu, India.

[2.] Department of Biotechnology and Bioinformatics, Sambalpur University, Odisha, India

[#]Authors have equal contributions

[*] Corresponding author: Dr. Debasish Mishra, email: res.mishra.d@gmail.com, debasish@vit.ac.in; ORCID: 0000-0002-1222-4656

Graphical Abstract:

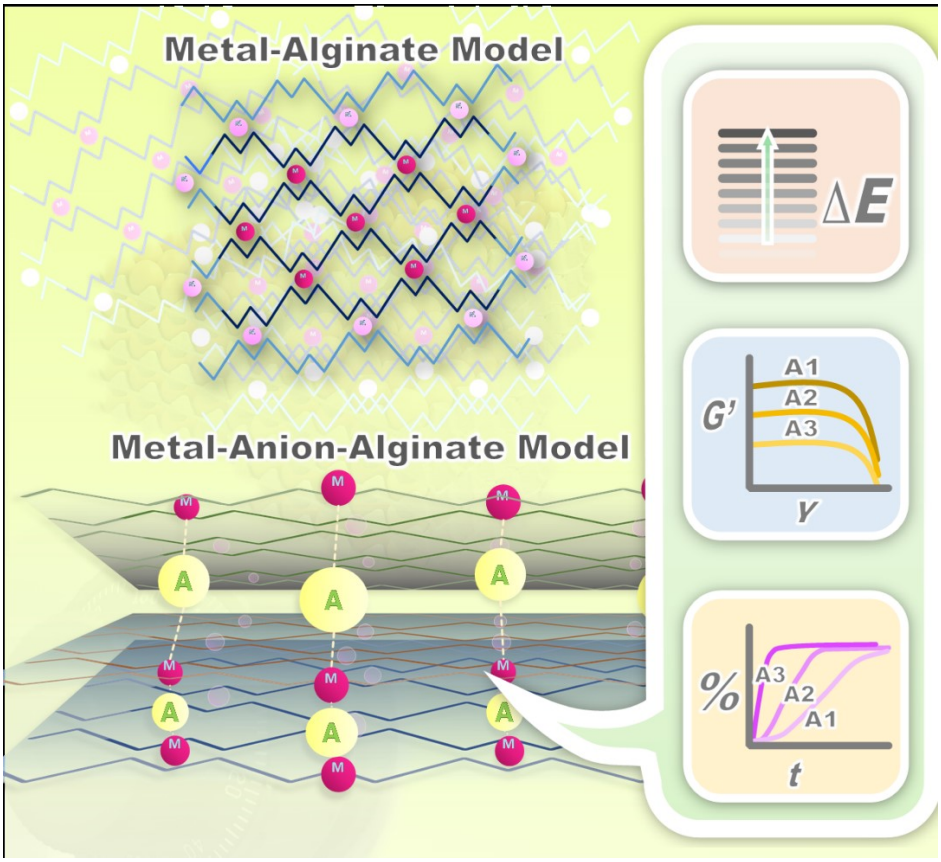

Description: *The article discovers unique way to fine tune the alginate hydrogel properties like viscoelasticity, drug-delivery, etc. via altering the anionic (A1, A2,..) counterpart of a divalent metal salt. As opposed to the conventional 'egg-box' like metal-alginate model, the authors propose an anion inclusive model i.e. metal-anion-alginate. The idea is based on compelling and novel evidences of anion-metal bonding and high interaction energy (ΔE) of overall molecular structure*

Research Highlights of the Article:

- Maiden and systematic attempt to study the role of anions in ionic gelation of sodium alginate.
- First spectroscopic evidences indicating both presence and interaction of anions in alginate gels and with the metallic counterpart, respectively.
- First study to systematically show anionic species dependent changes in visco-elastic properties and damping behaviours of the alginate gels.
- Unique attempt that shows anion dependent alteration in drug release profile and the release mechanisms in alginate beads.
- First attempt of DFT simulation study of metal-alginate complex that include anions as a part of the complex.
- Proposes substantiation of the renowned 'egg-box' model of metal-alginate to accommodate anions.

1. Introduction

In the era of modern synthetic polymers like acrylates and silanes, the world turned back towards sodium alginate for its biocompatibility and tuneable visco-elastic properties. Recent reports include attempts of organoids growth and differentiation employed tuneable visco-elastic property of alginate gels to obtain desirable responses [1,2]. Besides, alginate has been a favourite polymer for industries like - food [3,4], pharmaceutical [5,6], environmental bioremediation [7,8], biomedical device manufacturing [9], tissue engineering and 3D bioprinting [10], advanced physical and molecular therapeutic techniques [11]. Actually sodium alginate is a derivative of alginic acid which is a natural polysaccharide based biopolymer derived from brown algae (*Macrocystis sp.*). The monomeric units of the carbohydrate polymer are different uronic acids such as manouronic acids, guluronic acids, etc. in various combinations [12].

Most of the properties of alginates are attributed to their ionic crosslinking ability. It is still fascinating to observe sodium alginate solutions turning into a gel upon touching divalent or trivalent metal salt solution, viz. calcium chloride. The resultant gels are often referred as metal-alginate viz. calcium-alginate, aluminium alginate, etc. The viscoelastic property of the gel depends on the salt concentration as well as the cationic species [13]. For example cadmium or copper cations makes far too stronger alginate gels than that of calcium. In fact there are many reports that drew extensive charts on the gel forming abilities of various cationic species [12].

At a molecular scale, the gelation process is explained as transition of alginate polymer chains from a random orientation to an orderly egg box like configuration with the divalent ions. This arrangement is often called as 'egg-box' model [14]. It is assumed that the metal atom sits in the core and forms a 5 to 7 membered complex with the surrounding polymer chains. The model gets more substance when it was supported via x-ray crystallography, NMR, and computational modelling based studies [15,16]. The change in cationic species brings minor structural changes in the egg-box arrangement of metal-alginate complex. These tiny changes at molecular level are often attributed to huge variations in visco-elastic properties of alginate gels [17].

Revisiting the *in vitro* gelation process, it is initiated when sodium alginate solution is dropped into a salt solution that has both cations and anions. Role of cations were thoroughly understood since three-quarter of a century. However, the role of anions were hardly acknowledged. Even the famous 'egg box' model and its advancements never considered anions. Some school of thoughts believe that the anions, like chlorides in case of calcium chloride, normally get drained out during the washing steps of the hydrogels as soluble sodium chloride.

On a hindsight, anions were duly acknowledged in the scientific history for their role in dissolution and precipitation of macromolecules as early as 1878. Hofmeister clearly established that, anions along with their cationic counterpart of a salt could regulate the behaviour of proteins [18]. Alginic acid and derivatives are macromolecules as well. However, the role of anions in alginate gelation chemistry is rare explored. Even though it is clear that it would have vast applications.

Hence, it becomes more and more important to explore and explain the role of anions in alginate gelation. The present work is a systematic experimental and *in silico* study meant for understanding the roles of various anions in the ionic gelation of alginate. In order to achieve this, alginate gels and beads were fabricated using salts of various divalent cations viz. calcium, zinc and copper coupled with anions like chloride, acetate and sulphate. The biomaterials thus obtained were evaluated for their physico-chemical properties. In addition, a density function theory (DFT) based simulations of alginate-metal complex were further conducted to understand the roles of anions.

2. Results and Discussion

2.1. Anions have no role in gel densification but could affect bead size

2.1.1. Gelation time

Opacity or cloudiness has been an important indicator of gelation and gel densification [19]. In this case opacity of various alginate gel formulations were compared with respect to time and concentration of the gelling agent (Fig. 1a). In general, the opacity increases along with the salt concentration. Except for calcium sulphate, all salts having calcium and zinc cations reach their saturated opacity at 0.2 M concentration, which is representative of peak densification for that particular

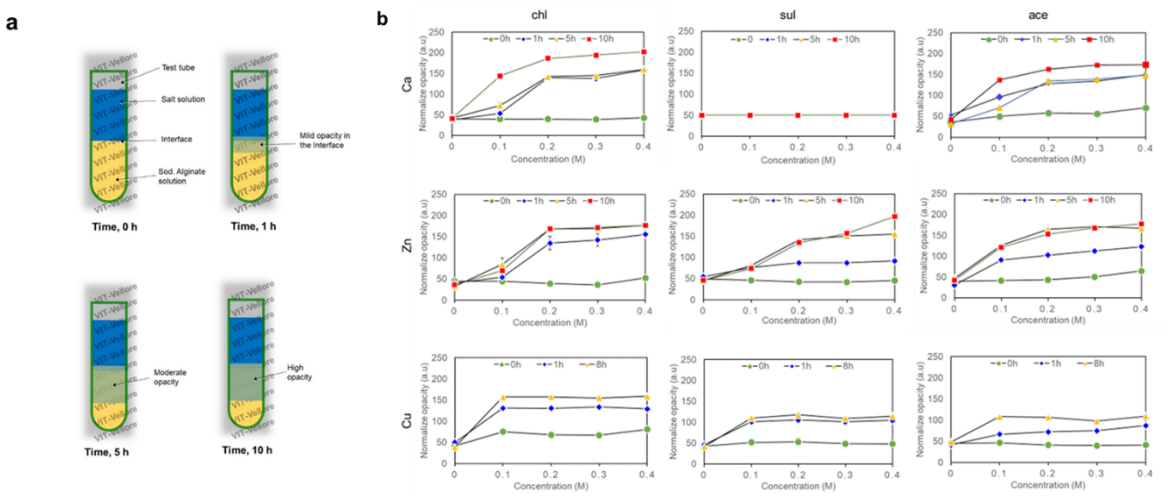

Figure 1. Gelation and densification. a) Cartoon of gel densification experiment. The sketches show test tube containing salt solution layered over alginate polymer solution, and temporal change in the interfacial opacity. The photographs of individual gels is shown in Fig. S1. b) Graphs showing time dependent changes in opacity of the alginate gels with various concentrations of different salts. The opacity of each gel was normalized with the opacity of the polymer solution before adding the gelling agents. Opacity is related to the magnitude of gelation.

concentration of salt solution (Fig. 1b). Calcium sulphate salt is least soluble among the group. Hence retained its particulate form in the interface of both the solutions, and could hardly bring any opacity or gelation. In case of copper salts, 0.1 M was adequate to completely achieve the plateau level. The calcium salts caused slower densification of the gels when compared to other two cations. Hence, it is indicative from the results that there was no apparent effect of anions in the gelation or gel densification of alginate hydrogels.

2.1.2. Bead size analysis

Beads appeared to be uniform and spherical with no tail whatsoever, for all composition, and the bead diameter ranged from 3.0-3.6 mm (Fig. 2 a,b). Largest average bead size was noticed in copper chloride salts, whereas the smallest size was that of calcium acetate beads. A common trend was observed. Sulphate anions resulted in smaller beads than that of chloride and acetate anions, in transition metal groups. According to the literature the average size of alginate beads created using dropping technique in calcium chloride solution are approximately 3 mm. However, this could vary with varying dropping rate and distance [20,21].

2.2. Change in anionic species alters the viscoelastic properties

2.2.1. Elastic Modulus

The viscoelastic properties viz. storage and loss moduli varies majorly with respect to the cations and subtly with respect to the anionic species (Fig. 3a). The moduli increased with the increasing salt concentrations, except for copper chloride and copper sulphate. Among cations the moduli increased in the following order, with copper leading the chart.

$$Cu >> Zn \geq Ca$$

The elastic moduli vary subtly but significantly with respect to anions when compared within a cationic group. The moduli increase was noticed in the following order, with sulphate anions clearly bottoming the chart under each cationic groups.

$$Acetate \geq Chloride > Sulphate$$

Similar trends for the role of cations in elastic moduli of alginate gels were reported in literature [13]. For the anions no systematic reports are available. However, just a decade earlier Lee and Rogers concluded that chlorides anions induces faster gelation of calcium alginate than di-carboxylate anions [22]. In this case we used a mono-carboxylate anion, i.e. acetate, and its gel strength was found superior to that of chloride anions. At least with calcium and copper counter-cations. In case of zinc the trend seems to derail

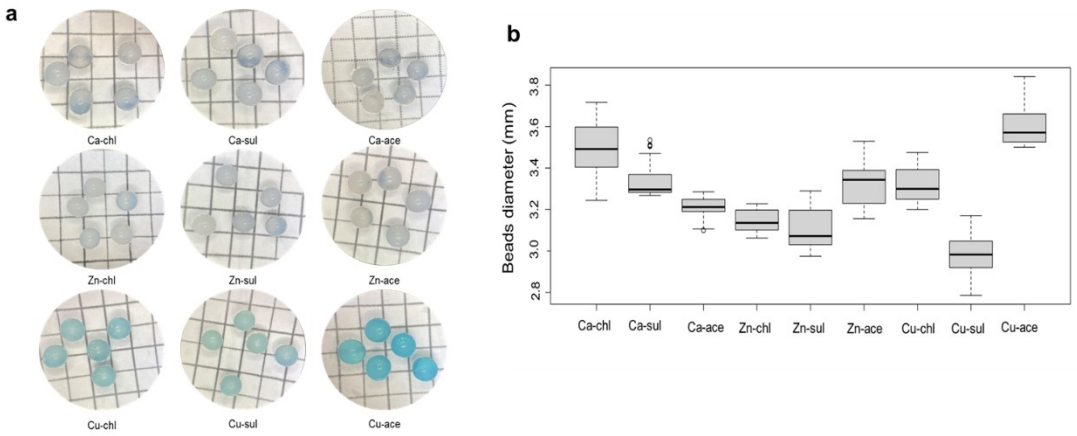

Figure 2. Characterization of alginate beads. Characterization of alginate beads. a) Photograph of sample alginate beads taken with the help of a stereo-zoom microscope aided with a 3 mm × 3 mm grid background. b) Box plot representing size distribution of different alginate beads. The midline that bisects the boxes is the median value (quartile Q2). The lower and upper edge of a box include data within quartiles Q1 and Q3, respectively. The whiskers represent the minimum and maximum data points. The outliers are represented as little circles.

possibly because of a complicated yet spontaneous zinc oxochloride formation chemistry that usually occur when zinc chloride is exposed in an aqueous medium [23]. Although it is mere indicative, but some recent reports supported our findings when they showed variations in the tensile and compressive strengths of alginate based films and beads with respect to anions [24,25].

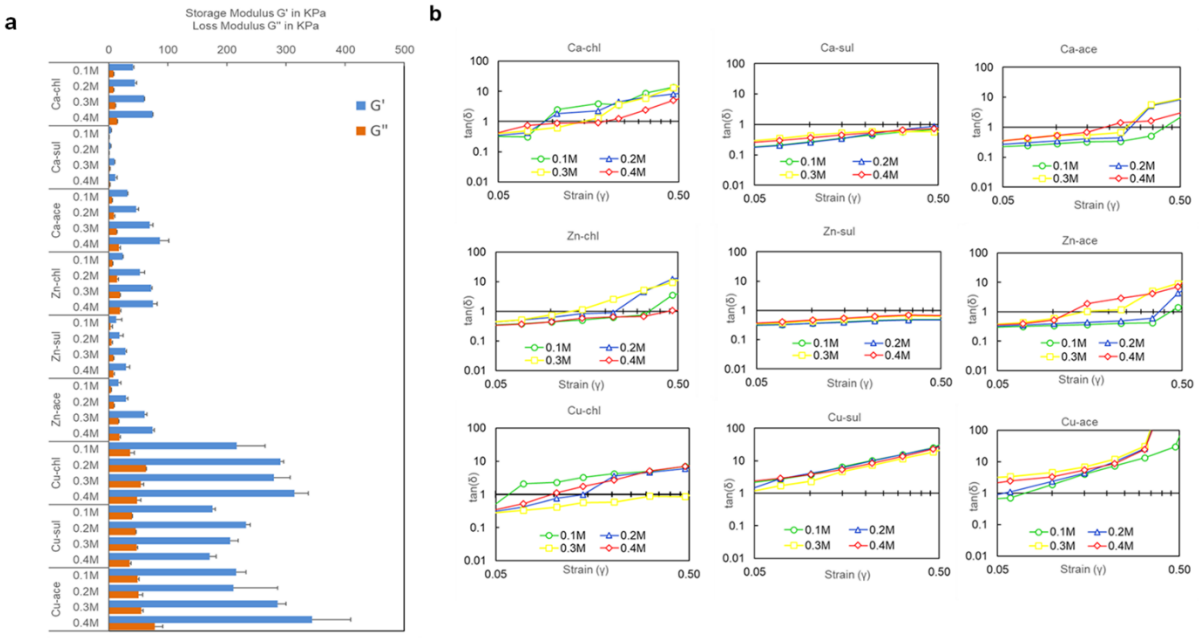

Figure 3. Rheological analysis. a) Histogram represents the storage modulus (G', blue) and loss modulus (G", red). The values are represented as mean ± standard deviation. b) Collage of scatter plots showing the loss factors (tan δ), aka damping factor or loss tangent, of various hydrogel formulations as a function of shear strain (γ), or deformation. The value of loss factor (tan δ) is usually determined as a ratio of loss modulus (G") to that of storage modulus (G') values at a particular strain value. The mid-line crosses Y-axis at unity, represents the transition point of elastic to viscous behaviour of the hydrogels. The magnitude of strain or deformation (γ) that brings elastic-to-viscous transition in a gel, could be called as critical - or transitional -strain. The term is analogously taken from the term 'glass transitional temperature', which is determined employing a similar methodology for thermolabile hydrogel materials.

2.2.2. Damping Factor

Although hydrogels are solids with substantial elasticity, often its elastic property shifts to viscous liquid like behaviour, when triggered with physical factors like stress, deformations, or temperature. This elastic to viscous transition is estimated via the damping factor (tan δ) values. When damping factor is plotted as a function of strain or deformation (γ), interesting findings were further recorded (Fig. 3b). Copper containing gels, although had highest storage moduli values, but they underwent transition at the least magnitude of deformation, indicating their plausible brittle property. On the anionic front, the sulphates showed atypical behaviours. Sulphates of calcium and zinc caused high reluctance in viscous transitions of the respective alginate gels at all concentrations and values of deformation. This is probably due to the cementing property of the said anion [26,27]. There was a time when hydrogels were mostly designed for the sole purpose of topical or oral drug delivery applications. Hence, their visco-elastic transitions hardly mattered to pharma industry of course with few exceptions [28]. When biomaterial applications of hydrogel peaked, its load bearing properties like visco-elasticity and damping ratios became an important concern. Recently biomaterial scientists understood that, tissue healing could be accelerated if the damping factors of an implanted hydrogel biomaterial and the host tissue matches [29]. Moreover with the advent of 3D bioprinting, damping factors for printed hydrogels has become a relevant factor to recognize their post-printing stability [30]. Lesser the damping factor, strudier is the hydrogel. Hence, it could be speculated among all the formulations acetate, and in some cases sulphate containing gels would be most suited for bioink application.

2.3. Spectral evidences of metal-anion bonding in presence of alginate

2.3.1. EDX

EDX analysis revealed that different anionic species influenced the uptake or retention of cations differently (Table 1). Per say, atomic percentage of calcium was highest with acetate anion containing alginate beads. Another interesting finding, sodium appeared in alginate beads of all calcium salts, and completely absent in zinc and copper beads. This observation was in line with earlier reports [17]. Generally when divalent or trivalent ions bind to alginate, it is assumed that sodium gets displaced from the polymer in free ionic form. Eventually sodium ions gets cleared up from the bead during repetitive washing steps. In this case, calcium possibly could not bind uniformly to the heteromeric alginate polymer chains, and leave pockets of un-displaced sodium ions [31].

2.3.2. FTIR

The signature region of the mid-IR (infrared) spectra revealed characteristic bands corresponding to carboxyl group of sodium alginate. Especially, the asymmetric-ν_{asym} (1596-1529 cm^{-1}) and symmetric - ν_{sym} (1400-1421 cm^{-1}) vibrational bands corresponding to the carboxyl group (COO^-) of alginate polymer [32]. According to literature, the band gap between the ν_{asym} and ν_{sym} vibrations of carboxyl group i.e. $\Delta\nu$ (COO^-) is

Table 1: Compilation of EDX elemental analysis data of various alginate bead formulations. The values depicted in the table are the mean ± standard deviation of atomic weight percentage of a particular element.

Atomic %age	Ca-chl	Ca-sul	Ca-ace	Zn-chl	Zn-sul	Zn-ace	Cu-chl	Cu-sul	Cu-ace
C	42.89 ± 1.2	40.13 ± 1.35	46.76 ± 6.54	40.47 ± 1.11	38.97 ± 6.06	39.29 ± 5.64	39.03 ± 3.18	22.08 ± 12.17	48.75 ± 6.78
O	46.11 ± 1.83	54.09 ± 2.57	48.22 ± 5.13	39.08 ± 3.77	49.2 ± 2.04	53.96 ± 4.14	44.74 ± 5.67	58.98 ± 9.07	42.03 ± 4.42
Na	2.56 ± 1.16	1.48 ± 0.2	0.1 ± 0.18	--	--	--	--	--	--
Cl	5.78 ± 0.42	--	--	10.35 ± 4.24	--	--	8.41 ± 3.35	--	--
Ca	2.67 ± 0.12	3.22 ± 1.7	4.92 ± 1.55	--	--	--	--	--	--
Zn	--	--	--	8.08 ± 2	11.11 ± 3.67	6.75 ± 1.64	--	--	--
Cu	--	--	--	--	--	--	7.81 ± 1.37	10.72 ± 2.79	9.21 ± 2.54
S	--	1.07 ± 0.64	--	--	0.12 ± 0.21	--	--	8.22 ± 0.85	--

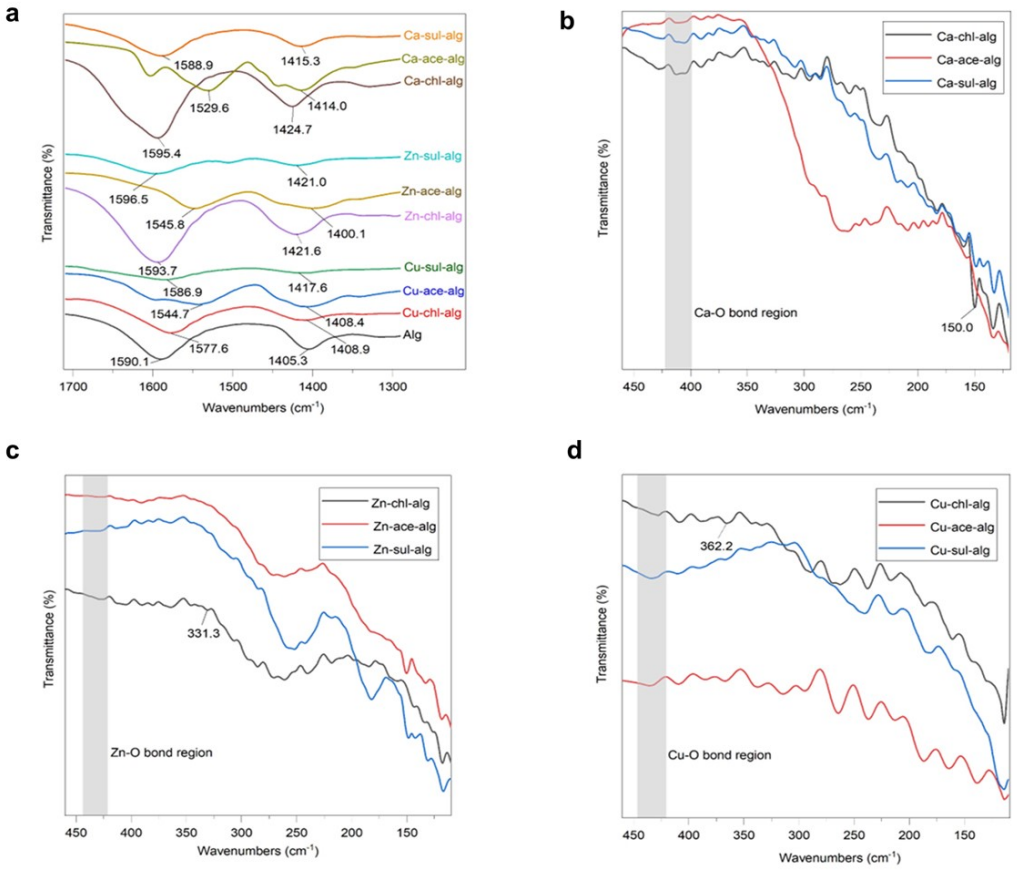

Figure 4. FTIR spectroscopy. a) FTIR spectrographs of various alginate dried gel beads. The graph shows the spectrum for mid-IR region, with an intent to identify vibration bands (*v1* and *v2*) for carbonyl groups, and other oxygen containing anions. According to literature, the minimum the difference between the bands, a better is the chance of complex formation between metal atom and oxygen atom of carbonyl group (Nakamoto 1987). A comparison of *v1* and *v2* band position is presented in a tabular form (Table S1). Bonding of other anions, especially non-oxygen containing anions like chloride, with the metal atom (M), could not be shown specifically via the mid-IR spectra. Hence, far-IR spectra was analyzed b) alginate gels of calcium salts c) zinc salts and d) copper salts. In all the graphs, a grey strip mark the M-O bond stretching bands (400 to 450 cm^{-1}). Unique bands that are possibly due to M-Cl interaction are indicated via arrow marks.

indicative of complex formation with metal atom. Lesser the band gap, stronger is the complex formation [33,34]. In the present case, pure sodium alginate, registered v_{asym} and v_{sym} bands at 1590.14 cm^{-1} and 1405.35 cm^{-1}, respectively, with a band gap i.e. Δv (COO^-) of 184 cm^{-1} (Fig. 4a, Table S1). Ionic gelation with divalent cationic salts caused a noticable reduction in the Δv (COO^-) values. However with respect to anions, the Δv (COO^-) seemed to follow the following order within the respective cationic groups.

Acetate < Chloride < Sulphate

It is clear that the complex formation is accentuated by the direct or indirect involvement of acetate ions [33,35–37]. Spectral scan of acetate salts alone was performed to rule out the possibility of pre-formed complexes (Table S2). The mid-IR spectral data indicated an active involvement of acetate anions. For tracing the involvement of other anions, far-IR spectra of the samples were analysed. According to literature, all terminal stretching metal-chloride bands were observed between 200 and 400 cm^{-1}. In this case, unique bands at 362, 331, and 150 cm^{-1} were observed in the dried alginate hydrogels containing chloride anions (Fig. 4b-d). In addition the vibrational band corresponding to metal-oxygen coordination bond between 400 to 450 cm^{-1}, was seen to augment in presence of acetate and sulphate anions, but stay levelled in case of chloride anions. This phenomenon was most pronounced in copper containing alginate beads (Fig. 4d). Far-IR and mid-IR spectroscopy provided evidences that all anions are involved in

complex formation via direct bonding with the metal atoms.

2.4. Anions influence water retention and drug release kinetics

2.4.1 Swelling and Desiccation

Dynamic swelling study revealed that all compositions absorbed water, except for calcium sulphate, and copper containing beads. About 40% and 60 % increase in weight was observed in calcium chloride and calcium acetate containing beads respectively, by the end of 24 h (Fig. 5a). Nearly, 30%, 60% and 160% increase in water content was observed in zinc chloride, zinc sulphate and zinc acetate containing beads, respectively. Among all formulations the highest swelling beads are that of zinc acetate, followed by zinc sulphate and zinc chloride containing beads. Interestingly, about 5% of weight loss was observed in calcium chloride beads within the first hour. However, later the mass kept on increasing. A similar phenomenon was observed in all zinc beads. Contrastingly, copper containing beads did not swell at all, instead they kept on losing mass persistently.

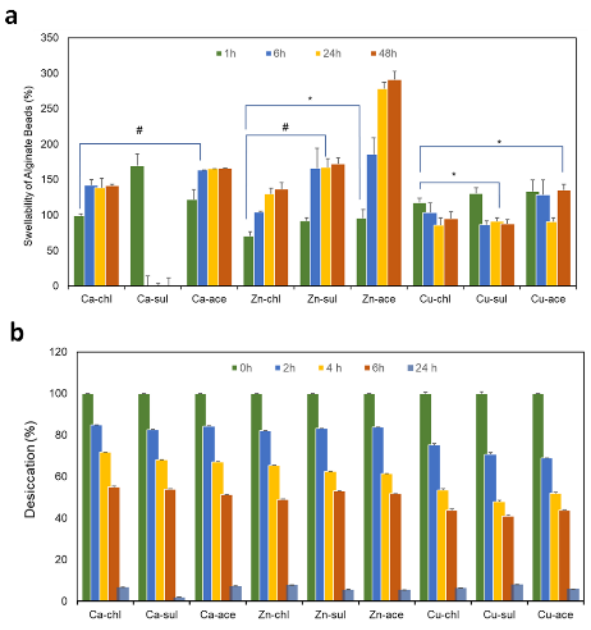

Figure 5. Swelling and Desiccation. a) Histogram represent swelling kinetics of alginate beads. The values are represented as mean ± standard deviation. Where '*' implies p-value < 0.05, and '#' indicates a p-value <0.001. b) Histogram showing the chronological weight loss of hydrated beads when subjected to desiccation in warm circulating air oven.

Copper beads were fast to desiccate as well when we focus at the 4 h desiccation data (Fig. 5b). Among anions, acetate lost the highest water content by 4h. In other words, acetate anion containing alginate beads were the quickest in absorbing and releasing water when compared to rest of the anions.

2.4.2. Drug Release

BSA was considered as a model protein drug for the release study. Most of the literature reported an encapsulation efficiency (E_E) of 5% to 40%. In the present work we report a maximum efficiency of nearly 15% pertaining to zinc acetate and minimum of about 12% in calcium chloride, zinc sulphate and copper sulphate [38]. The E_E of calcium acetate was moderately higher than calcium chloride beads However, the difference was statistically significant (Fig. S3i).

The cumulative drug release profile as depicted in Fig. 6a. According to data, the fastest to release 60% of BSA proteins was that of calcium-sulphate, within 1.5 h. Whereas, the slowest bead type to achieve the same was copper acetate i.e. in 72 h. Copper chloride and sulphate containing beads did not show any drug release beyond 33% and 2.5%, respectively till the maximum observation time. Similarly, calcium salts with various anions showed subtle yet considerable variations in the BSA releasing pattern. Although calcium chloride and acetate containing beads were capable of releasing 60% of their content within a close period of 7 h and 6 h, respectively. However, 80% of BSA release was achieved much faster by the chloride at 24 h, which was almost 10 h earlier than that of the acetate beads. The chloride containing beads showed burst release of BSA as early as 15 min, which may account for anomalous release behaviour but can justify the eventual accelerated pace of BSA release. Instances of similar burst drug release in calcium chloride containing alginate beads is already reported in literature [39]. In case of zinc salts, the sulphate containing beads were the last to release their 60% of content, by approximately 65 h. Whereas the acetate was the fastest in achieving the feat in just 6 h. Zinc chloride was moderately paced (12 h) in releasing the 60% of its content but, fastest in releasing 80% of the proteins in just 24 h. It is clear that with just varying the anions only one can get myriads of drug delivery options from the alginate gels. However, it would be further interesting to know the variations in the mechanism of

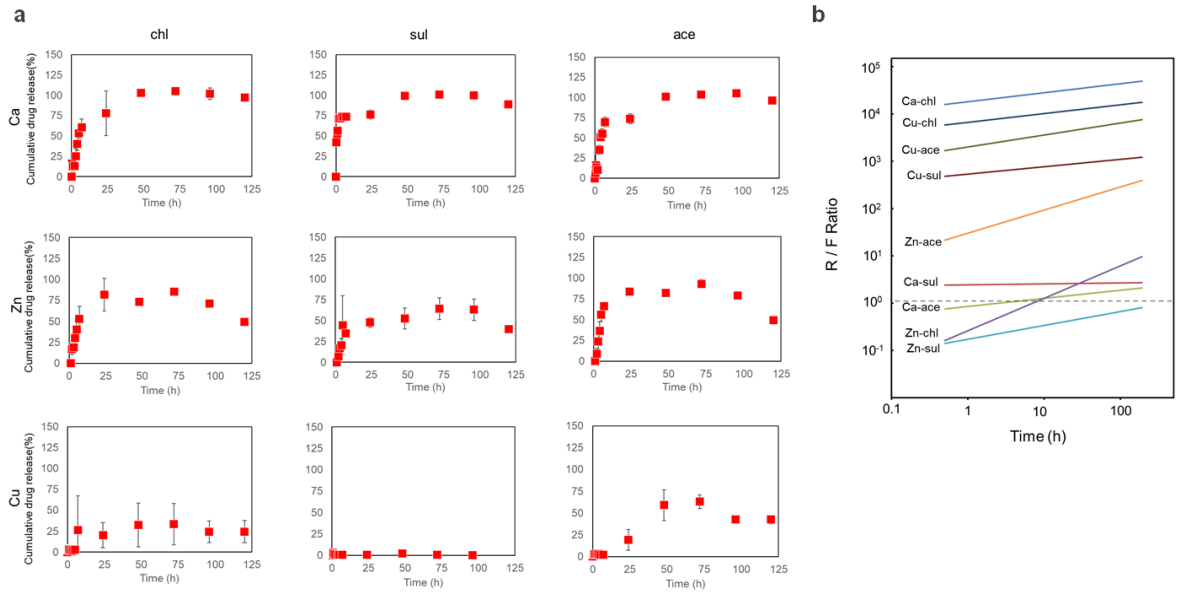

Figure 6. Drug release kinetics and model fitting. a) Cumulative drug (BSA) release profile of various alginate gel formulations, with respect to time. The drug released is represented as percentage of maximum drug loaded in the respective alginate gel formulations. The maximum drug loaded in the alginate gels is shown as drug loading efficiency in Fig. S2. The data is represented as mean ± standard deviation (n = 3). b) Graph represent the relation between the ratio of the drug release due to relaxation contribution (R) to that of Fickian contribution (F) and time. According to Peppas-Sahlin model, drug release from a hydrogel occur in two ways. Firstly, due to simple diffusion from the polymer network and secondly due to relaxation or stretching of the polymer network. The R/F ratio could predicts which mechanism is dominant at what point of time. Both the axes are in logarithmic scale. The dotted line indicates the mid-line (R/F = 1) whereby, the drug release is equally contributed by Fickian diffusional and relaxational modes. Meaning, diffusive drug release and polymer relaxation dependent drug release are identical. The profiles that lie below the mid-line show diffusion dominant drug release behaviour, whereas the ones lie above, follow a drug release mechanism that is mostly dependent on relaxation of polymer network. That may involve swelling based stretching of the network, or possibly disintegration of the networks via erosion of polymer molecules (individually or in bulk).

drug followed by different formulations of alginate gels.

2.4.3. Kinetic Model Fitting

Fitting the drug release profile to various kinetic models revealed the exact drug release mechanism followed by the various formulations. The fitting results showed that the Peppas-Sahlin (PS) model earned the highest coefficient of correlation, R^2 when compared with four other kinetic models [40]. Hence, it is pertinent that the best fit model to the experimental drug release data is the PS model. The original paper guided to estimate R/F ratio at various time points using the constant and exponent values, as shown in equation (3). The R/F ratio could predict the mechanism of drug release. Whether it has occurred through diffusion dominant (R/F ratio <1) or relaxation dominant (R/F ratio >1) fashion (Unagolla and Jayasuriya 2018). The R/F ratio in this case revealed that most of the BSA release seemed to be governed by polymer relaxation, with some exceptions (Fig. 6b). For example, zinc sulphate beads never showed relaxation mode of BSA release as the R/F ratio always stayed below the mid-line. Zinc chloride containing alginate beads unlike that of zinc sulphate, showed an initial protein release in a Fickian diffusion mode. However by end of the 7 h, relaxation mode started taking the lead. The acetate anions kept the zinc containing beads in the relaxation dominant zone. Although, the protein release was initiated with a lower relaxational mode which eventually scaled to moderately relaxational mode. Among calcium alginate beads, the anions again showed a drastic impact on the mode of drug release. Calcium chloride beads topped the chart with super-relaxational drug releasing behaviour. This could be due to certain level of erosion on the bead surface. Calcium sulphate beads came last in the same chart and hovered parallel to the mid-line. Calcium acetate beads however seemed to have started off the drug release with a diffusion dominant mode that slowly transited to a relaxation mode by the end of

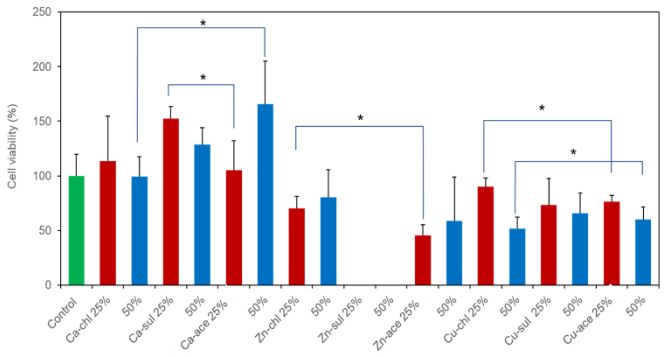

Figure 7. Cytotoxicity test. Cytotoxicity study with human breast cancer cell line (MCF7) in non-contact mode. The bar graph presents the results of MTT assay of cell viability after 24 h of exposure to various proportions of bead extracts (25% and 50%). The values are represented as mean ± standard deviation. Where '*' implies *p*- value < 0.05.

approximately 6 h. If we recall the drug release profile, by the same 6 h almost 60% of BSA is released from the calcium acetate alginate beads (Fig. 6a). This means close to 60% of drug was released in a diffusive mode. Diffusion based releases are more reliable and predictable hence are preferred than that of relaxational type release [41]. Hence, calcium acetate alginate beads were proved to be a more suitable candidate than calcium chloride alginate beads for drug formulations.

2.5. Anionic species could influence cytocompatibility of alginate biomaterials

The exposure of the bead extracts to mammalian cells revealed that the cell viability seemed to be compromised in presence of the extracts of zinc and copper beads (Fig. 7). In case of zinc, the acetate containing beads were found to compromise the cell viability more than that of chloride beads. Same trend was followed by copper chloride and copper acetate containing beads. Among calcium salts, none of the formulations were found to be cytotoxic. In most of the cases the viability reduced, when the extract fraction was doubled in the culture media (i.e. from 25% to 50%). Interestingly, calcium acetate containing alginate beads extract seemed to promote cell viability in a dose dependent manner. Moreover, the extracts could not be retrieved from zinc sulphate containing beads, as the dried homogenized beads turned into a thick jelly mass upon exposure to cell culture medium.

2.6. Computational models with anions are energetically more favourable

2.6.1. DFT studies

It is imperative from the second law of thermodynamics that systems with lesser energy tend to be more stable. Same implies for molecules, molecular interactions resulting in lowering the overall structural energy could be called as stable interactions. However, there is an unusual convention of calling more negative structural energy or interaction energy as higher than the less negative ones. In this case, first challenge itself was in computational modelling of the placement of metal atom in an alginate chain. The conventional idea of egg-box model had envisioned metal atoms in alginate polymer at position P, without concrete evidences (Fig. 8a,b). However, recent experimental evidence [16], and most recent computational modelling studies advocated that the metal atom is more suited to be placed at position Q [17,42,43]. Nevertheless, we conducted DFT studies at both the positions, and found that alginate dimers bind to metal ions with a slightly higher structural energy, when it was at position Q, meaning it was the most stable position. Hence considering our finding and earlier reports, we conducted rest of the DFT studies keeping metals at position Q (Fig. 8c). Out of various data obtained post-DFT optimization, interaction energies (ΔE) were compare estimating the stability of each structure. The ΔE is highest in alginate-copper (Alg-Cu), and followed by zinc and then calcium, when anionic species were not considered at all. The reason could be found via electron localization function (ELF) study (Fig. S4). Ligand moieties from alginate dimer interact via electrostatic mode with calcium. These interactions had larger interatomic distances and are considered weak. Whereas, in case of zinc and copper the interactions are strong coordination type with shorter interatomic distances. The trend is consistent with previously reported DFT studies [17,42–44]. The interaction energy of calcium containing structures were the least followed by zinc and copper. Similar simulation results were reported elsewhere [45]. When anions were considered, the comparison of interaction energies (ΔE) revealed that the metal-anion-alginate structures have higher ΔE values than that of the complexes without anions viz. metal-alginate (Fig. 8a). The highest interaction energy was recorded in the case of acetate anions. Moreover, sulphates of all metals had the least interaction energies among their respective cationic group. On the other hand, ΔE per novel bond formation, in complexes with both cation and anions, were found to be lesser than the complexes with cations only (Fig. 9b). According to the literature, the general stability of a molecular structure depends on the overall structural energy value rather

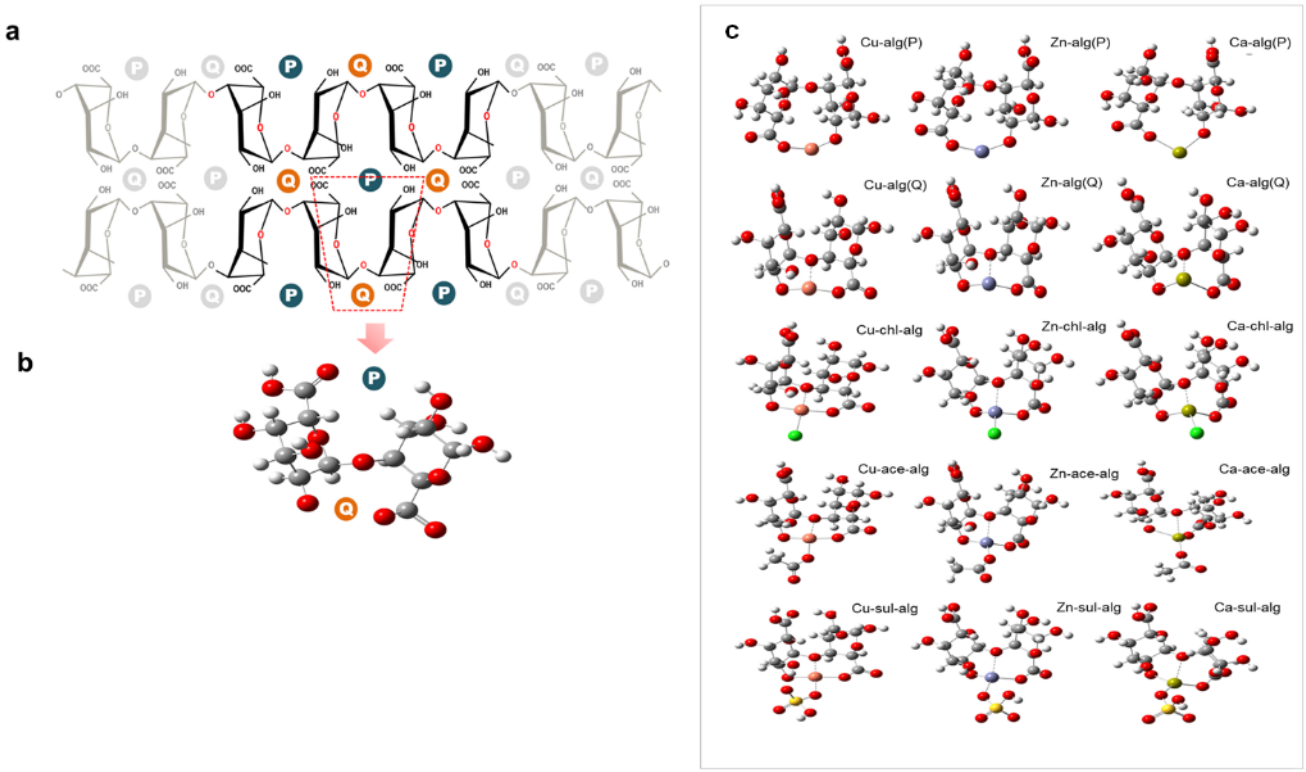

Figure 8. DFT simulation. The 'egg-box' model of metal-alginate interaction. a) The 2D schematic representation of alginate, guluronic acid rich zone, showing two possible positions, 'P' and 'Q', where, metal atom can sit and suitably interact with the polymer chains apparently in an 'egg-box' like arrangement. b) 3D optimized alginate dimer structure in which 'P' and 'Q' positions were indicated. c) Collage alginate-complex structures as obtained from DFT based optimization. Three structures in the first row represent copper alginate (Cu-Alg), zinc alginate (Zn-Alg) and calcium alginate (Ca-Alg) optimization structures that have metal atom at position 'P' of alginate dimer. Second row: optimization structures of aforesaid complexes having metal at position 'Q' of alginate dimer. The DFT study revealed, position 'Q' is energetically more favourable than that of position 'P'. The third row represents the DFT optimization structures that include anions as an integral part of the complex. Chloride anion with different alginate complexes viz. copper chloride alginate (Cu-Chl-Alg), zinc chloride alginate (Zn-Chl-Alg) and calcium chloride alginate (Ca-Chl-Alg) were depicted in the third row. Fourth and fifth rows show involvement of acetate and sulfate anions, respectively, in their DFT optimization structures. Colours of different atoms as represented in the DFT optimization structures- carbon:grey, hydrogen: white, oxygen: red, copper: peach, zinc: greyish-blue, calcium: dark yellow, chlorine: green, and sulphur: yellow. The white lines represent firm interactions or bonds between atoms, and the dotted line represent weak interactions.

than individual bond energies [45,46]. Another noteworthy finding is that, the anionic contribution to the ΔE values in calcium salt containing structures ranged from 22-30%. Whereas for copper salts the anionic contribution was as low as 12-13% only. Hence, from the simulation results it could be deduced that anions have detrimental role in the hydrogel properties when paired with calcium counterions, but will have minimal role in when paired with copper counterions. The trend deduced hereby surprisingly fits the storage modulus profile (Fig. 4a).

2.7. Discussion

Considering the EDX data and DFT results side by side, it becomes imperative that copper and zinc cations interacted with alginate polymer very strongly, and possibly that is the reason it could replace all the sodium ions, and hence it did not show up in EDX spectra. However, there were traces of sodium in EDX spectra of calcium containing alginate beads. From DFT studies we found that calcium interact weakly with alginate, this may be another reason why calcium could not replace sodium completely during alginate gelation. It is understandable that the ions interacting with the alginate polymers are retained in the hydrogel network, even though it is just sodium ions. EDX spectra showed representative atoms of all the anions, in all formulations of the beads. It means, anions could interact with the alginate polymer chains directly or indirectly. Furthermore FTIR data revealed that, anion

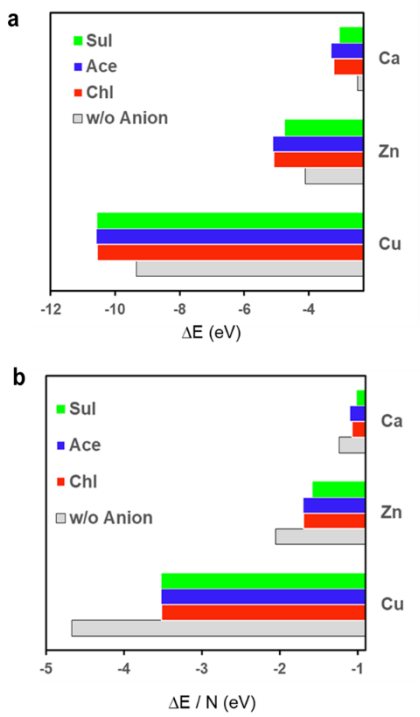

Figure 9. Interaction energy. a) Histogram of interaction energies, ΔE, of complexes without and with anions as integral part of the complex. b) Histogram of ΔE calculated per new bond formed (N).

show unique spectral signatures related to direct anion-metal bonding (Fig. 4a-d). Then, there were significant increment of interaction energy values in presence of anions as revealed by DFT studies, which indicated that anions bind to the metal ions instead of directly binding to the alginate polymer chain. At the molecular level, this is a strong evidence that anions actively participate in the alginate metal complex formation (Fig. 9a).

Coming to the anion driven hydrogel properties, we found some intriguing correlations. Fig. 10a presents a summary of both cation and anion related alginate gel properties studied in the present work. Properties like damping factor, swelling and mechanism of drug release seems to be correlate positively. For example in the case of acetate anion, alginate beads were the quickest to swell and desiccate in their respective cationic groups. Hence, they could absorb and release water effortlessly. Such properties are indicative of a porous monolith like drug delivery vehicle. This feature correlates to high strain dependency for phase transitions in acetate containing hydrogels. It in turn correlates to prevalence of diffusive mode of drug release, a signature mode of release in monoliths, from acetate anion containing alginate gels [47]. While discussing the properties it is important to mention that recent independent studies reveal that change in the anionic species alone could alter the bead-textural, compressive and tensile moduli, optical, gustational, enzyme immobilization, and metal absorption properties of alginate hydrogel [20,22,24,25,33,36]. Anions are so important for alginate gelation that, Pérez Madrigal and co-workers claimed to develop alginate hydrogel beads using anions alone, in their acidic form. Meaning the cationic counterpart was hydrogen ion or hydronium ion [48]. It is noteworthy that the group never discounted the role of resident sodium ions. Hence, it is in fact both cations and anions that hold the alginate network in place in a hydrogel.

Certain hydrogel properties like storage modulus could be related to interaction energy, ΔE values derived from DFT simulation (Fig. 3 and Fig. 9). For example the storage moduli of sulphate containing hydrogel were always the least in its respective cationic groups, and the trend is the same with its ΔE value. Overall, it could be said that the *in silico* DFT simulation results helped in substantiating the experimental data in many ways, and greatly helped in proving the importance of anions in the ionic gelation of alginate. However, chemical interactions are often unpredictable which could create mismatch in the *in vitro* and *in silico* data trends. Experimentation with a larger set of anions and cations could lead to further clarification in future.

Hofmeister series for anions is based on their kosmotropic or chaotropic properties. Which in turn are based on the hydration, solubility, atomic and ionic radii like attributes. Among the anions under considerations, sulphate is listed the first, whereas, chloride and acetate appear in the middle of series. However, our findings presented some contrasting trends. This could be explained in two ways. Firstly in this case alginate, which is a purely acidic polymer, is considered that share no similarities with proteins molecules. Secondly, the interaction of the ions possibly and factually occurs due to steric facilitations and structural energy minimization, as evident from *in silico* studies. However, this is only a pilot study aimed to establish the importance of anions in alginate gelation. As mentioned earlier a large scale study considering numerous anions would enable to recreate an elaborate series in the line of Hofmeister's work, which will help biomaterial scientists to choose the right kind of salts with right type of cations and anions

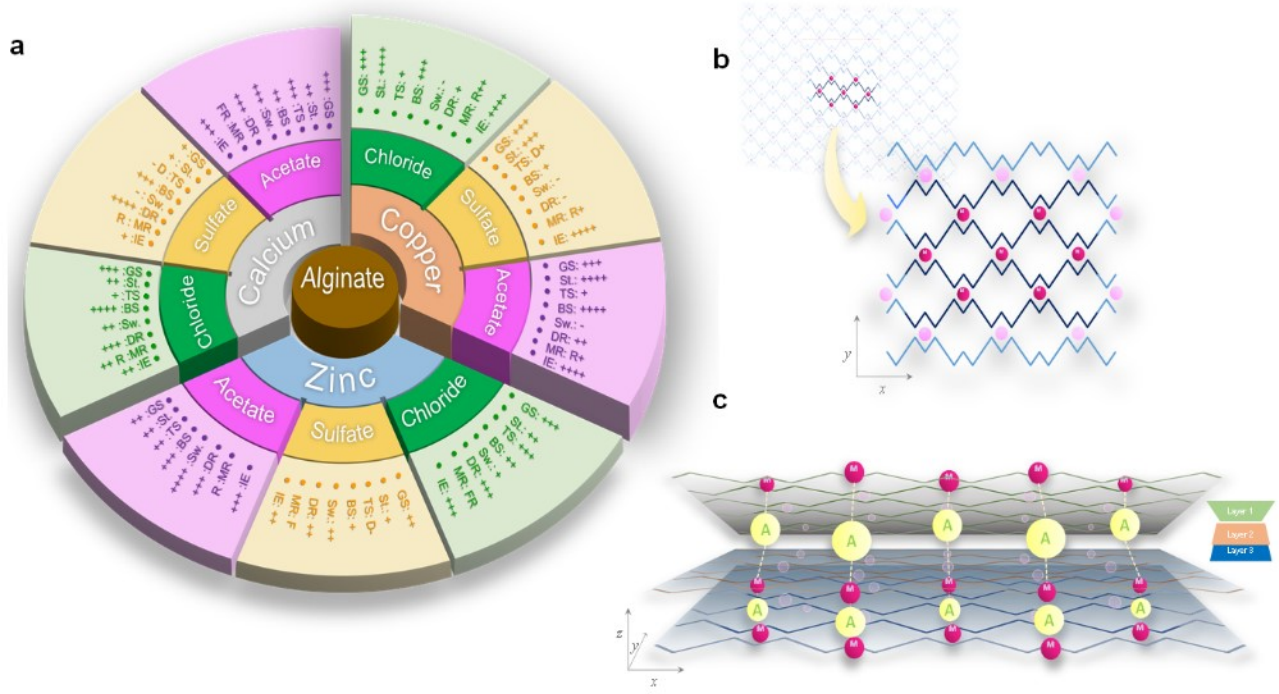

Figure 10. Summary of anion driven properties of alginate gels and the plausible reason. a) A radial segmentation Infographics (*aka* pie-chart type schematic), showing a summary of anion dependent properties of alginate gels. Copper containing gels are represented by the tallest slices, indicating their highest storage moduli and fast gelation speed. The abbreviations and the scores are as follows: 'GS' is gelation speed which could be slow (+)/ medium (++) / fast (+++); 'St.' is strength that in turn is represented by storage modulus and is scored as low(+)/ medium (++) /high (+++) / very (++++); 'TS' is transitional damping strain is scored as low (+) / medium (++) / high (+++) strain transitions, in addition, there are cases of no transitions at all, whereby the scoring is done based on the damping profile that always stayed either above (D+) or below (D-) the mid-line. 'BS' is bead size that could be small (+)/ medium (++) / big (+++) / biggest (++++). 'Sw.' is the swellability of the beads. The material could lose weight in swelling medium (-), if it swells, the weight increase could be low (+) / medium (++) / high (+++) / very high (++++). 'DR' is cumulative drug release. It could be close to zero (-) / slow (+)/ medium (++) / fast (+++)/ very fast (++++). 'MR' is mode of drug release. This could be diffusional (F) / relaxational but close to midline (R) / moderately relaxational (R+) / super-relaxational or possibly erosional (R++) / Diffusional mode turning to relaxational mode (FR). 'IE' is theoretically obtained interaction energy (ΔE) values which could be very low (+) / low (++) / medium (+++)/ high (++++). b) Artistic representation of how alginate polymer (green, rust red, blues lines) bind to metal atoms (pink, M) and form extended pattern of 'egg boxes' in two dimensions. c) Artistic representation of our hypothesis that, the stacks of the said 2D sheets are held in z-axis via anions (yellow, A). The dotted yellow lines represent the interaction between the metal atoms and anions, which are perpendicular to the alginate-metal coordination or complexation plane.

for extracting desirable hydrogel properties from sodium alginate.

It would not be fair if the 'egg-box' model of metal-alginate complex formation is not discussed before concluding this article. The findings of the present paper substantiates the model in many ways. However, we believe that the egg-box model fairly explains formation of two dimensional sheets or strips of metal-alginate complexes (Fig. 10b). Anions provide additional interaction facets that possibly could help in stacking up the metal-alginates sheets in the third dimension (Fig. 10c).

3. Conclusion:

To date, most of the alginate ionic gelation has been planned with a cation centric idea. Our work radically changes this notion. It brings anions to the centre stage. The work not only elaborates on the anion dependent drastic change in gel properties but also shows how anions are indispensable for alginate hydrogel formation at structural and energetic levels. Especially we propose a theory based on the results, how the anions place themselves in the z-axis without disturbing the egg-box grid of metal-alginate complex. In conclusion, the first of its kind, systematic *in vitro* and

in silico study brought many counterintuitive facts about alginate gels as summarized in Fig. 10a. Cations are grossly and anions are subtly responsible for alginate hydrogel properties. Properties like elastic moduli, bead size, swelling, desiccation, drug delivery fraction and modes, and cytocompatibility were shown to be influenced by anions. It was found that alginate gels of calcium acetate will have superior properties than that of calcium chloride. Highest swelling gels had zinc acetate and not zinc chloride. Zinc chloride gels were the most disciplined and showed diffusion dominant drug delivery mode, and there are many more interesting findings. Changing anions seems to have opened up a new portal of opportunities for biomaterial scientists, especially for their bioink development endeavours. Our group is working on extending the list of anions. We invite other interested research groups to join hands in our endeavour. Lastly, from now on it may not be exaggerating if alginate ionic gels are described not only with their cations but also with their counter-anions viz. calcium-chloride-alginate instead of calling it calcium-alginate.

4. Experimental Methods

Materials: Sodium alginate was procured from Sigma-Aldrich. Calcium chloride dihydrate ($CaCl_2.2H_2O$), Calcium sulphate dihydrate ($CaSO_4.2H_2O$), Calcium acetate monohydrate ($Ca[CH_3COO]_2.H_2O$), Zinc chloride anhydrous ($ZnCl_2$), Zinc sulphate heptahydrate ($ZnSO_4.7H_2O$), Zinc acetate dihydrate ($Zn[CH_3COO]_2.2H_2O$), Cupric chloride ($CuCl_2$), Copper sulphate ($CuSO_4.5H_2O$), Copper acetate ($Cu[CH_3COO]_2.H_2O$), Bovine Serum Albumin (BSA), and other fine chemicals were procured from HiMedia, Mumbai.

Ionic gelation of sodium alginate: Ionic gelation was conducted using two distinct methods to obtain a hydrogel bead and a gel slab. Hydrogel beads were obtained by controlled dropping technique as described elsewhere [20]. Briefly, 2% w/v solution of sodium alginate was dropped at a steady flow rate of 1 mL/min using a syringe pump (Pump Elite 11, Harvard Apparatus), from a height of 8 cm into a 0.2 M salt solution bath [21]. The bath is constantly stirred at 300 rpm at room temperature, in order to obtain consistent sized beads. The beads allowed 30 min maturation time before they were washed in distilled water for further experimentations.

Gel slabs were obtained using a customized 3D printed mould, 60 mm diameter [49]. Aqueous sodium alginate solution 2% w/v, was poured into the mould, layered with salt solution soaked filter papers at its base. The alginate solution was further topped with a similar salt soaked filter papers. The contraption was left in a moist environment at room temperature for 12 h or until, the sandwiched alginate sol was transformed into a hydrogel slab.

Gelation time and gelling concentration: Ionic gelation process of aqueous sodium alginate is usually accompanied with the increment of opacity of the sol state. The experiment is intended to study the time dependent gelation dynamics in terms of the altering opacity of the gels. Approximately 2 ml of aqueous sodium alginate solution (2% w/v) was poured in series of test tubes. Equal volume of salt solution with varying molarity (0.1 - 0.4 M) were gently overlaid upon alginate solution. Following the addition, the transition of opacity was observed, in the interfacial zone, with respect to time, and photographed for further image analysis. The opacity of the interface was quantified as mean grey intensity values using NIH imageJ software.

Beads size estimation: Beads thus formed were observed under a stereomicroscope (Luxeo 2S, LABOMED). A 3 mm grid was placed beneath the beads for reference measurements. The bead size was measured using NIH imageJ software. The data were represented using box plots.

Swelling study: Swelling study of alginate beads was conducted according to the literature [50]. Briefly, alginate beads were air dried and were allowed to swell in phosphate buffer (pH 7.2) at room temperature in separate containers. The swelling percentages were calculated as follows.

$$\%_S = \frac{W_f - W_0}{W_0} \times 100 \ldots\ldots\ldots (1)$$

Where, W_f is the final weight of the beads, W_0 is the initial weight of the beads. For estimation of desiccation capabilities of the beads, freshly prepared beads were taken and were allowed to desiccate in a hot air oven (60 ºC), until there is no further loss in weight. The weights were measured intermittently, and the percentage desiccation was calculated using a similar equation.

Drug Release: BSA was used as a model drug for the drug release study. The appropriate amount of BSA

(1.5% *w/v*) was added to the 2 % *w/v* sodium alginate aqueous solution and was thoroughly mixed [47]. Beads were made as described in the earlier section. Approximately 2 g of beads were suspended in 19 ml of release medium i.e. phosphate buffered saline (PBS pH-7.2).

The drug release profile was evaluated in a cumulative mode. Briefly, 1ml of release media was extracted at set time periods and the BSA protein content was estimated in each fraction via Bradford assay as described elsewhere [51]. Fig. S3(ii) shows the distinctive chromogenesis during Bradford assay, in the presence of copper salt.

Drug Encapsulation Efficiency: Freshly prepared BSA-alginate beads were subjected to quick and complete dissolution in phosphate buffered saline (PBS pH-7.2) spiked with a powerful chelating agent, i.e. EDTA (2 M). The released BSA was quantified using Bradford assay. The following equation was used to calculate total encapsulation efficiency [52].

$$E_E = \frac{C_t}{C_p} \times 100 \text{ …….. (2)}$$

Whereby, E_E is the encapsulation efficiency (%), C_t is theoretical amount of BSA that should be present in a given mass of beads, and C_p is actual amount of BSA that is present in a given mass of beads.

R/F ratio: Constants and exponents obtained from Peppas-Sahlin model fitting to drug release profile *viz.* k_D, k_R and m, could be used to estimate a ratio of relaxational to that of Fickian contribution towards drug release via the following equation [40].

$$\frac{R}{F} = \frac{k_R}{k_D} t^m \text{ …….. (3)}$$

When, R/F ratio >1, the polymer relaxation dominates the drug release, if R/F >> 1, it could be polymer super-relaxation (sometimes seen as erosion), however, if R/F <1, it is Fickian diffusion [41].

Rheology: The alginate gel slabs were casted with a dimension of 25 mm diameter and 2 mm thickness. The 8 h matured slabs were subjected to analysis in a plate-on-plate type rheometer (Anton Paar MCR 95). Briefly, an amplitude sweep test was run at a fixed oscillatory speed of 10 rad/s, with a variable angular strain ranging from 0.01 to 100%. The storage (G') and loss (G") moduli were estimated from the linear visco-elastic region (LVER) of their respective curves. The average value of the moduli were plotted in MS excel as a function of salt type and concentration. Whereas, the damping factor or loss factor (tan δ) was plotted as a function of angular strain or shear strain, γ (Fig. 2b).

Energy Dispersive X-Ray analysis: The elemental analysis of the beads were performed via energy dispersive X-Ray (EDX) unit (OXFORD instrument) which is attached to a scanning electron microscope (EVO/18 from ZEISS). Beads were sliced into half, followed by air drying. Further the beads were sputter-coated with palladium, and observed under electron microscope (Fig. S2). Randomly selected areas were scanned for EDX based elemental analysis (Table 1).

Fourier Transformed Infra-Red (FTIR) Spectroscopy: Air-dried beads were crushed to a fine powder. The powders of various bead compositions were scanned in Agilent Cary 630 FTIR Spectrometer, and transmission intensity data were collected in the range 4000–650 cm^{-1} wavenumbers [11]. It could be noted that, the equipment is advanced yet compact, and does not need KBr pellet substrates to embed the powder samples. Nevertheless, a minimum of 1000 scans were considered for generating one spectrum for any given sample. Far IR- FTIR spectroscopy was carried out in Thermo Nicolet iS50 instrument that allows spectral scan from 700 to 100 cm^{-1}. Finally the spectral data were analysed and plotted with the help of Origin 11 software.

Cytotoxicity: Cytotoxicity test was conducted following the methodology described in ISO 10993-1 with minor modification. Modifications such as choice of cell line and time period of extraction. Human cell line, MCF7 was considered, instead of murine L929 cells, for studying the cytotoxic properties of alginate beads in non-contact yet extraction method. Briefly, about 0.5 g of beads were thoroughly crushed to coarse powder form. The powder was further soaked in 2 ml of DMEM cell culture media supplemented with 10% serum for 4 h at 37 ºC. The media was filtered with a 0.22 micron syringe filter, and added directly to 96 well culture plate that was pre-seeded with 10^5 cells/ ml of MCF7 cells and allowed to attain 80% confluence. After 24 h of incubation, the cell viability was estimated using MTT assay a previously established methodology.

Density Functional Theory Simulation: In order to understand the relevance of anions at a molecular scale, density functional theory (DFT) based *in silico* study

was performed using Gaussian 16. Briefly, guluronate dimer was drawn in GaussView 6.1, followed by selection of optimization methods that included DFT subtype B3LYP functional with a basis set selected as LANL2DZ in aqueous environment as reported elsewhere [53]. The said optimization process returned the lower energy confirmation of the input dimer, which is further considered as the representative of the guluronic acid rich portion, *aka* GG block, of alginate polymer. The optimized dimer structure is subjected to further optimization steps with divalent cations only, and cation-anions jointly in separate runs. The optimized output structures were visualized in GaussView for structural energy, and other reactivity parameters. Electron localization function (ELF) analysis was conducted in Multiwfn 1.9 using the same optimization output files. [43,46,53]

Interaction energy: The interaction energy (ΔE) of a molecular complex was determined by subtracting the structural energies of the participating entities from that of the structural resultant molecular complex, using the following equation [54,55]. The structural energy data of each molecular complex was obtained after DFT optimization.

$$\Delta E = E_{A,B\ldots,n} - (E_A + E_B + \cdots + E_n).. \quad (4)$$

Where, $E_{A,B,\ldots,n}$ is the structural energy of the complex i.e. dimer-M or dimer-M-anion complex, whereas, E_A, E_B, … till E_n are the respective structural energies of participating entities such as alginate dimer, metal ion, anion, etc.

Statistical Analysis and Model Fitting: All the data points represent the mean values of the data set and the error bar represent the standard deviation. In order to compare the data sets in Student's t-test was employed with minimum sample size, n = 3. If the p value obtained was less than 0.05, the difference was considered significant. Statistical box plot for comparing the bead size using 'boxplot()' function in R programming language. For kinetic model fitting to drug release profiles, the cumulative release data of upto 60% release was considered. The profile was fitted with various kinetic models one by one using the in-built solver tab in MS Excel 2013, and, using a specially designed MS excel add-in i.e. DDsolver [56]. The best fitting data were selected on the basis of the adjusted correlation coefficient (R^2) values, and represented in the form of a table (Table S3).

Acknowledgements:

Authors are grateful to Dr. Thirumoorthy Krishnan, associate professor, department of chemistry for providing valuable technical suggestions. Authors also acknowledge Mrs. Chitra Kaliachelvan, assistant professor (senior), department of horticulture and food science for her immense support in rheological studies. Authors are profusely thankful to Dr. Vijayakumar D., professor, department of electrical engineering for providing access to their supercomputer facility for the *in silico* studies. The authors initiated ionic gelation and crosslinking of alginate while working on DST-SERB sponsored grant (sanction no. ECR/2017/001325). Hence they profusely thank department of science and technology−science and engineering research board (DST-SERB), government of India for their support. Lastly, the authors would like to acknowledge the VIT management to support the project in terms of finance, infrastructure and logistics.

Research Data

Research data will be made avalilable upon genuine request.

Conflict of Interest

The authors declare no conflict of interests.

References

[1] A. Elosegui-Artola, A. Gupta, A.J. Najibi, B.R. Seo, R. Garry, C.M. Tringides, I. de Lázaro, M. Darnell, W. Gu, Q. Zhou, D.A. Weitz, L. Mahadevan, D.J. Mooney, Nat. Mater. 22 (2023) 117–127.

[2] D. Indana, P. Agarwal, N. Bhutani, O. Chaudhuri, Adv. Mater. 33 (2021) 2101966.

[3] Y. Qin, J. Jiang, L. Zhao, J. Zhang, F. Wang, in: Biopolymers for Food Design, Elsevier, 2018, pp. 409–429.

[4] T. Senturk Parreidt, K. Müller, M. Schmid, Foods 7 (2018) 170.

[5] A. Dalmoro, A.A. Barba, G. Lamberti, M. Grassi, M. d'Amore, Adv. Polym. Technol. 31 (2012) 219–230.

[6] M. Szekalska, A. Puciłowska, E. Szymańska, P. Ciosek, K. Winnicka, Int. J. Polym Sci. 2016 (2016) 1–17.

[7] A. Sinha, K.K. Pant, S.K. Khare, Int. Biodeterior. Biodegrad. 71 (2012) 1–8.

[8] Y. Zvulunov, A. Radian, ACS EST Water 1 (2021) 1837–1848.

[9] L. Peng, Y. Liu, J. Huang, J. Li, J. Gong, J. Ma, Eur. Polym. J. 103 (2018) 335–341.

[10] Sardelli, Lorenzo, Tunesi, Marta, Briatico-Vangosa, Francesco, Petrini, Paola, Soft Matter 2021 (2021) 8105–8117.

[11] C. Thomas-Busani, J.A. Sarabia-Sainz, J. García-Hernández, T.J. Madera-Santana, L. Vázquez-Moreno, G. Ramos-Clamont Montfort, RSC Adv. 10 (2020) 28755–28765.

[12] A. Haug, B. Larsen, in: Proceedings of the Fifth International Seaweed Symposium, Halifax, August 25–28, 1965, Elsevier, 1966, pp. 271–277.
[13] C. Ouwerx, N. Velings, M.M. Mestdagh, M.A.V. Axelos, Polym. Gels Networks 6 (1998) 393–408.
[14] G.T. Grant, E.R. Morris, D.A. Rees, P.J.C. Smith, D. Thom, FEBS Lett. 32 (1973) 195–198.
[15] C.A. Steginsky, J.M. Beale, H.G. Floss, R.M. Mayer, Carbohydr. Res. 225 (1992) 11–26.
[16] P. Sikorski, F. Mo, G. Skjåk-Bræk, B.T. Stokke, Biomacromolecules 8 (2007) 2098–2103.
[17] J. Brus, M. Urbanova, J. Czernek, M. Pavelkova, K. Kubova, J. Vyslouzil, S. Abbrent, R. Konefal, J. Horský, D. Vetchy, J. Vysloužil, P. Kulich, Biomacromolecules 18 (2017) 2478–2488.
[18] P. Jungwirth, P.S. Cremer, Nature Chem 6 (2014) 261–263.
[19] A. Maltais, G.E. Remondetto, R. Gonzalez, M. Subirade, J. Food. Sci. 70 (2005) C67–C73.
[20] B.-B. Lee, P. Ravindra, E.-S. Chan, Chem. Eng. Technol. 36 (2013) 1627–1642.
[21] Z.Q. Li, L.D. Hou, Z. Li, W. Zheng, L. Li, AMR 648 (2013) 125–130.
[22] P. Lee, M.A. Rogers, Int. J. Gastron. Food Sci 1 (2012) 96–100.
[23] T. Yamaguchi, S. Hayashi, H. Ohtaki, J. Phys. Chem. 93 (1989) 2620–2625.
[24] F.V. Cendon, B.B. Salomão, R.M.M. Jorge, A.L. Mathias, Colloid. Polym. Sci. 299 (2021) 693–703.
[25] I. Choi, Y. Lee, J.S. Lyu, J.S. Lee, J. Han, Food Hydrocolloids 131 (2022).
[26] G. Frigione, in: Advances in Cement Technology, Elsevier, 1983, pp. 485–535.
[27] P.W.R. Osinaga, R.H.M. Grande, R.Y. Ballester, M.R.L. Simionato, C.R.M. Delgado Rodrigues, A. Muench, Dent. Mater. 19 (2003) 212–217.
[28] L. Hahn, M. Beudert, M. Gutmann, L. Keßler, P. Stahlhut, L. Fischer, E. Karakaya, T. Lorson, I. Thievessen, R. Detsch, T. Lühmann, R. Luxenhofer, Macromol. Biosci. 21 (2021) 2100122.
[29] M. Bartnikowski, R.M. Wellard, M. Woodruff, T. Klein, Polymers 7 (2015).
[30] L. Cacopardo, N. Guazzelli, R. Nossa, G. Mattei, A. Ahluwalia, J. Mech. Behav. Biomed. Mater. 89 (2019) 162–167.
[31] I. Braccini, R.P. Grasso, S. Pérez, Carbohydr. Res. 317 (1999) 119–130.
[32] S.K. Papageorgiou, E.P. Kouvelos, E.P. Favvas, A.A. Sapalidis, G.E. Romanos, F.K. Katsaros, Carbohydr. Res. 345 (2010) 469–473.
[33] U. Vaid, S. Mittal, J. Nagendra Babu, React. Funct. Polym. 97 (2015) 48–55.
[34] K. Nakamoto, Infrared and Raman Spectra of Inorganic and Coordination Compounds, John Wiley & Sons, Inc., Hoboken, NJ, USA, 2008.
[35] R.D. Mounts, Tetsuya. Ogura, Quintus. Fernando, Inorg. Chem. 13 (1974) 802–805.
[36] T. Pan, Y.-J. Sun, X.-L. Wang, T. Shi, Y.-L. Zhao, Chin. Chem. Lett. 25 (2014) 983–988.
[37] J.E. Tackett, Appl. Spectrosc. 43 (1989) 483–489.
[38] T. Suksamran, P. Opanasopit, T. Rojanarata, T. Ngawhirunpat, U. Ruktanonchai, P. Supaphol, J. Microencapsulation 26 (2009) 563–570.
[39] M. Witzler, S. Vermeeren, R.O. Kolevatov, R. Haddad, M. Gericke, T. Heinze, M. Schulze, ACS Appl. Bio Mater. 4 (2021) 6719–6731.
[40] N.A. Peppas, J.J. Sahlin, Int. J. Pharm. 57 (1989) 169–172.
[41] J.M. Unagolla, A.C. Jayasuriya, Eur. J. Pharm. Sci. 114 (2018) 199–209.
[42] Y. Abdellaoui, C.A. Celaya, M. Elhoudi, R. Boualou, H. Agalit, M. Reina, P. Gamero-Melo, H.A. Oualid, J. Mol. Struct. 1249 (2022) 131524.
[43] C.S. Ardiles, C.C. Rodríguez, Arabian J. Chem. 14 (2021) 103325.
[44] D. Hari, A. Kannan, Mater. Today Proc. 62 (2022) 1532–1543.
[45] P. Agulhon, V. Markova, M. Robitzer, F. Quignard, T. Mineva, Biomacromolecules 13 (2012) 1899–1907.
[46] C. Menakbi, F. Quignard, T. Mineva, J. Phys. Chem. B. 120 (2016) 3615–3623.
[47] H. Kaygusuz, F.B. Erim, React. Funct. Polym. 73 (2013) 1420–1425.
[48] M.M. Pérez-Madrigal, J. Torras, J. Casanovas, M. Häring, C. Alemán, D.D. Díaz, Biomacromolecules 18 (2017) 2967–2979.
[49] E.A. Growney Kalaf, R. Flores, J.G. Bledsoe, S.A. Sell, Mater. Sci. Eng., C. 63 (2016) 198–210.
[50] G. Pasparakis, N. Bouropoulos, Int. J. Pharm. 323 (2006) 34–42.
[51] A. Nochos, D. Douroumis, N. Bouropoulos, Carbohydr. Polym. 74 (2008) 451–457.
[52] N.C. Hunt, A.M. Smith, U. Gbureck, R.M. Shelton, L.M. Grover, Acta Biomaterialia 6 (2010) 3649–3656.
[53] L. Bekri, M. Zouaoui-Rabah, M. Springborg, M.S. Rahal, J. Mol. Model. 24 (2018) 312.
[54] M. Elhoudi, R. Oukhrib, C. A. Celaya, D. G. Araiza, Y. Abdellaoui, I. Barra, Y. Brahmi, H. Bourzi, M. Reina, A. Albourine, H. Abou Oualid, J. Mol. Model. 28 (2022) 37.
[55] S.A. Ivanov, I. Arachchige, C.M. Aikens, J. Phys. Chem. A 115 (2011) 8017–8031.
[56] Y. Zhang, M. Huo, J. Zhou, A. Zou, W. Li, C. Yao, S. Xie, AAPS J 12 (2010) 263–271.

Please download the "Supplementary Information File" to access supplementary tables and figures, e.g. Table S1, S2…. and Fig. S1, S2,…..

~End of the Document~